Experimental Study on Sealing Performance and Flow Characteristics of Magnetic Fluid in Extremely Tiny Clearance under Magnetic Field

M. Motozawa[1], Y. Kato[2], W. Rakpakdee[1], M. Fukuta[1]

[1]Faculty of Engineering, Shizuoka University, Shizuoka, Japan
[2]Graduate School of Integrated Science and Technology, Shizuoka University, Shizuoka, Japan
Email: motozawa.masaaki@shizuoka.ac.jp

Sealing performance and flow characteristics of magnetic fluid in extremely tiny clearance less than 10 μm under magnetic field are investigated experimentally. The clearance in the test section is set to 15, 20, 30 and 50 μm in addition to the extremely tiny clearances of 5 and 10 μm, and magnetic field is applied to magnetic fluid flow at the clearance. The results show that 1.2 MPa of maximum pressure resistance was obtained at 5 μm of extremely tiny clearance from the pressure resistance test for high viscosity magnetic fluid, and the relationship among frictional coefficient, magnetic field and Re is quite different among 5, 20 and 50 μm of tiny clearance from the flow characteristic test.

Keywords: Magnetic Fluid, viscosity, nanoparticles.

1. Introduction

A magnetic fluid is a colloidal dispersion of ferromagnetic nanoparticles in carrier liquids such as water, kerosene, oil and so on. The diameter of inner magnetic nanoparticles of magnetic fluid is about 10 nm, and is small enough to have magnetic single domain. The magnetic fluid can be treated as a Newtonian fluid under no magnetic field, and it is well known that it has possibility to control flow characteristics actively by magnetic body force by application of the magnetic field because the magnetic fluid keeps fluidity as if strong magnetic field is applied to the magnetic fluid. Therefore, many applications by using magnetic fluid is proposed. For instance, in the thermal engineering field, Philip et al. [1] measured thermal conductivity of a magnetic fluid containing Fe3O4 nanoparticles and

reported about 300 % of thermal conductivity improvement was obtained at 7.8 vol% of particles concentration. On the contrary, in the tribological field, Chouhan et al. [2] conducted tribological test using a ferromagnetic lubricating oil containing Fe3O4 nanoparticles. They reported that wear was reduced about 35 % compared to the base oil. Thus, many applications of magnetic fluid were proposed and part of them are in actual use now. One of the successful and practical applications of magnetic fluid is the magnetic fluid seal [3-8]. Magnetic fluid seal has the advantage of long life without damage due to the small wear compared with general mechanical seals.

As sealing technologies are very important in many fields, there are a lot of studies on the characteristics of magnetic fluid seal. van der Wal et al. [5] proposed a new type magnetic fluid rotary seal which has a magnetic fluid replenishment system in the sealing ring while sealing capacity is maintained, and this seal has 69.8 kPa of static sealing capacity for air in clearance of 100 μm. Li et al. [6] provided a reference for designing magnetic fluid seal in liquid environment, and this seal has 28.5 kPa of static sealing capacity in water in clearance of about 100 μm. Jiang et al. [7] represented magnetic fluid seal with stepped pole pieces, and this seal has 180 kPa of static sealing performance against air pressure in clearance 100 μm. Mitamura [8] proposed a magnetic fluid seal for implantable blood pumps, and the pressure resistance for liquid was 49.2 kPa in clearance of 50 μm. Table 1 lists the clearance and pressure resistance in previous researches of magnetic fluid seal. As listed in this table, most of studies on magnetic fluid seal have been conducted under the condition that the clearance of magnetic fluid seal is hundreds of microns and the pressure resistance of single seal is not so large (tens kPa order).

On the other hand, a compressor is important component in several mechanical systems. In many cases, as compressor consumes large part of the total energy in the system, improvement of the efficiency in the compressor directly leads to the energy saving. To improve the efficiency in compressor, it is necessary to reduce the leakage of compressed gas in compressor. Because leakage of compressed gas directly affects the compressor performance, several sealing technologies have been proposed [9]. For instance, a tip seal is often used to the sliding parts of scroll compressor for preventing the leakage, and Fukuta et al. [10] investigated the mechanism of the tip seal from the viewpoint of leakage and friction.

Table 1 Review of the pressure resistance and clearance in magnetic fluid seals.

Author	Notes	Clearance μm	Maximum pressure resistance kPa
Mizutani et al. [4]	Single stage Double stages	100-200	32.4 62.2
van der Wal et al. [5]	Double stages	100	69.8
Li et al. [6]	Double stages	100-700	28.5
Jiang et al. [7]	Stepped seal	100	180
Mitamura [8]	Double stages	50	49.2

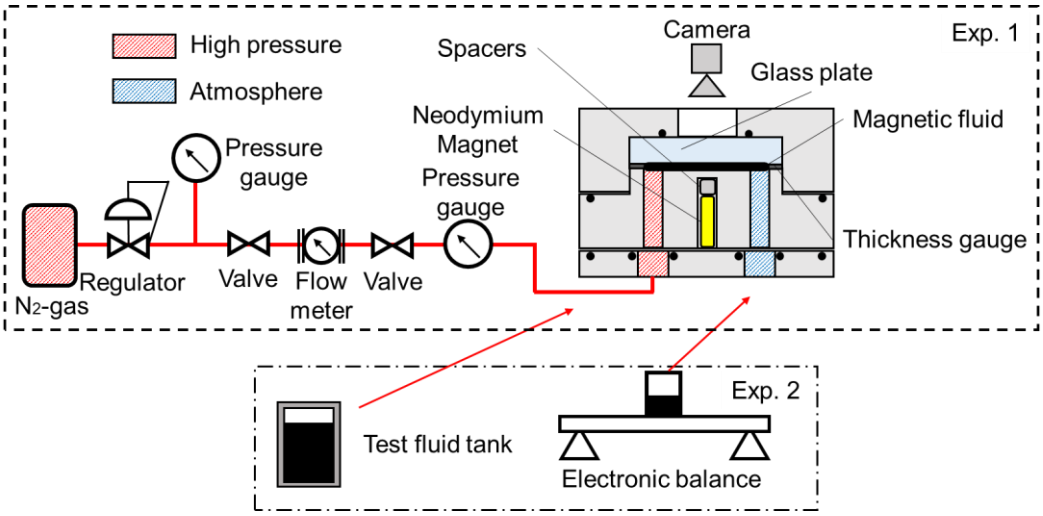

Fig. 1 Experimental apparatus.

In this study, we consider that sealing technology of magnetic fluid would apply to the sliding part of compressor. Generally, the clearance of the sliding part of compressor is around few microns, and high-pressure resistance (e.g. MPa-order in some cases) is required. If the sealing technique of the magnetic fluid can be applied to such an extremely tiny clearance (around few μm) and high-pressure condition (around 1 MPa), the application of magnetic fluid seal becomes expanding more. Moreover, it seems that the flow characteristics of magnetic fluid is different in such an extremely tiny clearance. However, because the situation is quite different from the normal magnetic fluid sealing listed in Table 1, there are few studies on the sealing performance and flow characteristics of magnetic fluid in extremely tiny clearance.

In this present study, both the sealing performance (Exp. 1) and flow characteristics (Exp. 2) of magnetic fluid in extremely tiny clearance less than 10 μm are investigated experimentally. Experiment was carried out by using a micro-channel flow path which has 15, 20, 30 and 50 μm of clearance (i.e. channel height) in addition to 5 and 10 μm of extremely tiny clearance, and magnetic field is applied at the clearance.

2. Experimental Apparatus and Procedure

Figure 1 shows the overview of experimental apparatus for Exp.1. Experimental apparatus consists of nitrogen cylinder, regulator, flowmeter and the test section. In the case of Exp. 2, the test fluid tank and electronic balance are installed at upstream and downstream of the test section, respectively. The detailed structure of the test section is shown in Fig. 2 (a), and the same test section is used in both Exp. 1 and Exp. 2. The test section consists of bottom plate, middle part, sight glass, and glass holder. Flow path which has extremely tiny clearance is formed by sandwiching a thickness gauge as a spacer between the middle part and sight glass. The clearances h (i.e. channel height) can be set to 5, 10, 15, 20, 30 and 50 μm by changing thickness gauge, and channel width and length are 10 mm and 20 mm, respectively as shown in Fig. 2(b). Magnetic field can be applied at the center of the tiny clearance by

embedding a permanent magnet in a magnet groove under the tiny clearance. The detailed condition and experimental procedure in Exp. 1 and Exp. 2 are explained below.

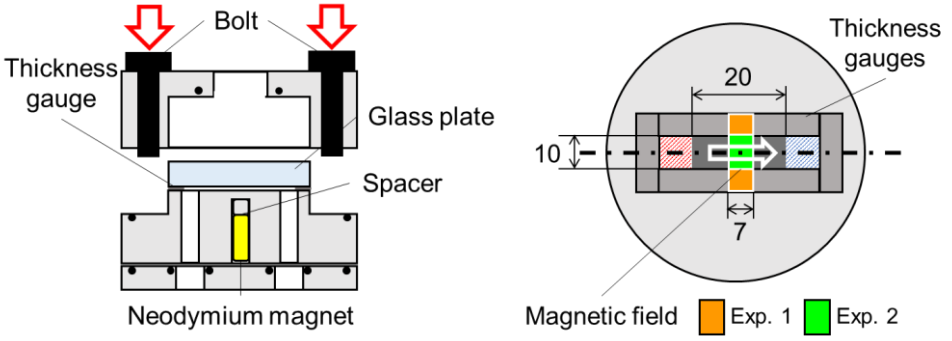

(a) (b)

Fig. 2 Test section; (a) detailed structure and (b) top view of sealing surface.

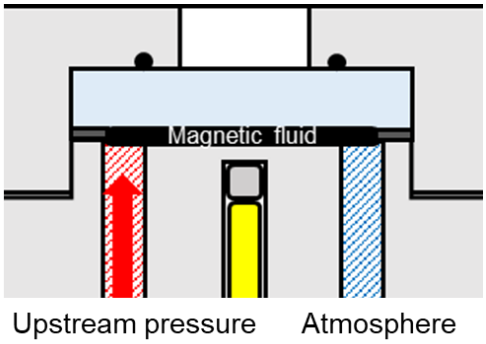

Fig. 3 Cross-section of the test section in Exp. 1

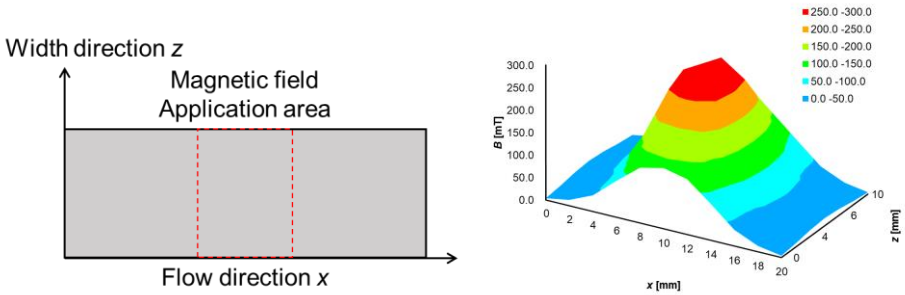

(a) (b)

Fig. 4 Magnetic field in Exp. 1; (a) Magnetic field area and (b) magnetic field distribution for 300 mT

2.1. Details in Exp. 1

Figure 3 shows the cross-sectional diagram of the test section in Exp. 1. Extremely tiny clearances are set to 5 and 10 μm in the Exp. 1. Magnetic fluid is provided and held at the extremely tiny clearance before the experiment, and then pressure starts to be applied to the clearance of the test section from the nitrogen cylinder. The maximum pressure, at which the seal breaks and leakage starts to occur, is measured, and when leakage occurs the process of leakage development is observed from the upper slight glass. Upstream pressure is applied to magnetic fluid for 180 s, and increases by every 0.05 MPa. The magnetic field intensity is 0 mT (no magnetic field) and 300 mT. Magnetic field application area and magnetic field distribution in the test flow path are shown in Fig.4 (a) and (b), respectively. The maximum magnetic field (300 mT) is obtained at the center of the sealing surface, and magnetic field intensity gradually decreases to the upstream and downstream of the center of the magnetic field area.

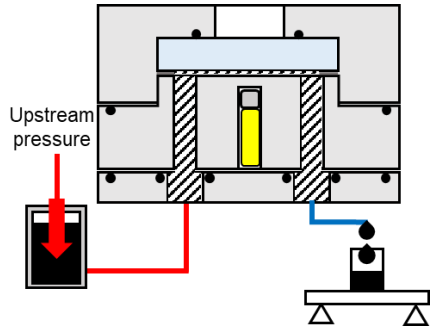

Fig. 5 Cross-section of the test section in Exp. 2.

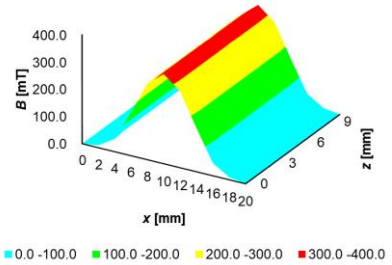

Fig. 6 Magnetic field distribution in Exp.2 for 330 mT.

2.2. Details in Exp. 2

Figure 5 shows the cross-sectional diagram of the test section in Exp. 2. Tiny clearances (i.e. channel height) are set to 5, 10, 15, 20, 30 and 50 μm in the Exp. 2. To avoid errors due to reassemble of the test section, the exact value of channel heights are determined by calibration with using the standard liquids for calibrating viscometers (JS 2.5 produced by NIPPON GREASE Co.,Ltd.) before each experiment. After the calibration, the inside of the test section is cleaned by flowing the ethanol through the flow path. The test magnetic fluid is filled in the tank which is located at the upstream of the test section, and the test magnetic fluid flows through the channel in the test section by upstream pressure applied from the nitrogen cylinder. Mass flow rate is measured by weighing method with using the electronic balance at the downstream of the test section. The magnetic field intensities are 0 (no

magnetic field), 54.4, 102.6, 136.3 and 330 mT, and magnetic field distribution is shown in Fig. 6. This figure indicates that the magnetic field in the spanwise direction of the channel is almost uniform, and the magnetic field gradually decreases to the upstream and downstream of the center of the magnetic field area same as Exp. 1.

Table 2 Physical properties of test magnetic fluids.

Sample	Base	Viscosity Pa・s	Density kg/m^3	Saturation magnetization mT	Experiment
A	Poly-α-Olefin	0.06	1267	48.5	Exp. 1
B	Alkyl benzene	0.65	1357	49.5	
C	Alkyl benzene	0.85	1339	50.2	
D	Kerosene	0.0055	1332	58.6	Exp. 2

2.3. Test magnetic fluids

Three test magnetic fluids A, B and C which have different base fluids and viscosities are used in Exp. 1, and kerosene-based magnetic fluid is used in Exp. 2. These test magnetic fluids were prepared by Ferrotec Material Technologies Co., and their physical properties are listed in Table 2. The viscosities of magnetic fluid in this table were measured by ourselves with using a rheometer.

3. Results and discussion in Exp. 1

3.1. Time-series variation of leakage flow

Figures 7 and 8 show the typical result of the time-series variation of the leakage flow rate and pictures of the process of leakage occurrence. The horizontal axis in Fig. 7 is the elapsed time after the application of upstream pressure. As shown in Fig.7, just after the application of upstream pressure, the leakage flow rate increases immediately, and then the flow rate becomes zero. This is because air flow occurs quickly by the upstream pressure but the magnetic fluid works as a seal the air flow stops in the flow system. If leakage does not occur, the flow rate would not change and is zero during experiment. When leakage occurs, a leak flow path develops in the flow channel with breaking seal. However, the flow rate does not change in the initial stage of leakage occurrence because leak path develops in seal point. After that, the flow path reaches the outlet of the flow channel and the leakage flow rate increases. We classified these features into three stages as (a) no leakage, (b) initial stage of leakage, (c) leakage as shown in Fig. 7, and the typical pictures in these stages are shown in Fig. 8.

In this study, the retention time of magnetic fluid seal in the flow channel is defined as the time from the upstream pressure application to leakage occurrence, and if the retention time is longer than 180 seconds we judged no leakage occurs under the given pressure condition.

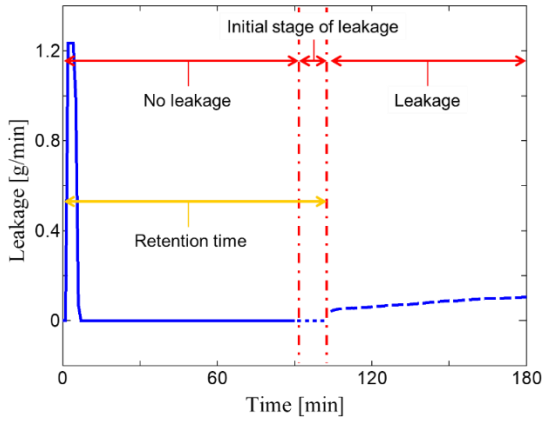

Fig. 7 Time-series variation of leakage mass flow rate.

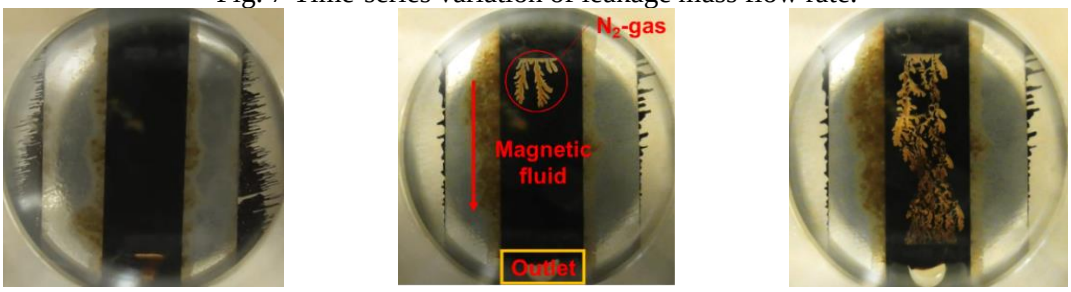

(a) (b) (c)

Fig. 8 Typycal pictures in the process of leakage occurrence ; (a) No leakage, (b) Initial stage, and (c) Leakage

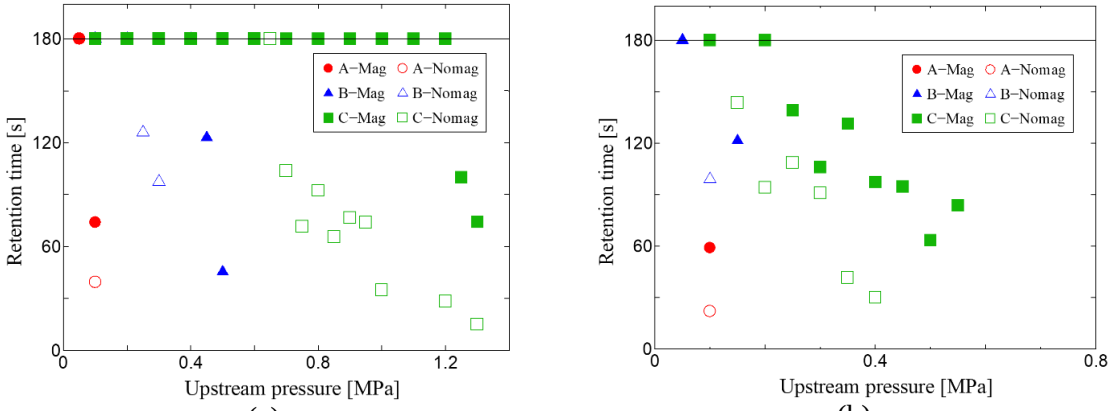

(a) (b)

Fig. 9 Relationship between retention time and upstream pressure for (a) 5 μm and (b) 10 μm of extremely tiny clearances.

3.2 Pressure resistance of magnetic fluid seal

Figure 9 shows the relationship between the retention time and upstream pressure for (a) 5 μm and (b) 10 μm of the extremely tiny clearances. In these figures, the closed and open plots are with and without magnetic field to magnetic fluid seal in the flow channel, respectively. These figures clearly indicate that the retention time of magnetic fluid becomes

long for large viscosity magnetic fluid, and increases by applying magnetic fluid because the magnetic fluid works as a seal. In addition, the retention time becomes shorter by applying large upstream pressure. Thus, the maximum pressure at which no leakage occurred is defined as a pressure resistance in this study.

Table 2 Pressure resistance (Exp. 1)

Condition	Sealing performance MPa	
	5 μm	10 μm
A-Mag	0.05	<0.05
A-Nomag	0.05	<0.05
B-Mag	0.4	0.1
B-Nomag	0.2	<0.05
C-Mag	1.2	0.2
C-Nomag	0.65	0.1

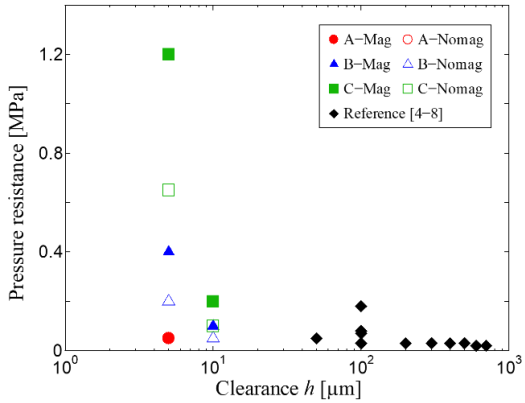

Fig. 10 Relationship between pressure resistance and seal clearance.

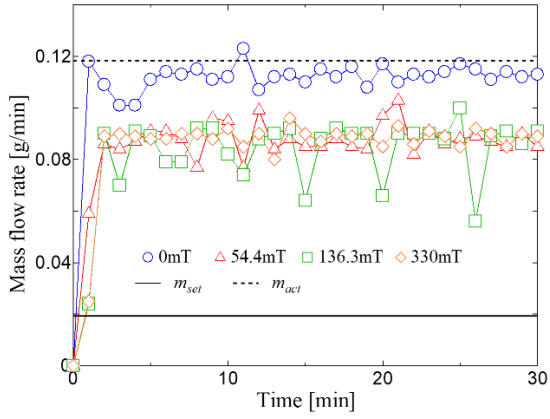

Fig. 11 Time-series variation of mass flow rate of magnetic fluid flow for 5 μm of clearance.

Table 2 lists the pressure resistance obtained, and Fig. 10 shows that relationship between

pressure resistance and seal clearance compared with the references [4-8]. These results indicate that the pressure resistance drastically increases in the extremely tiny clearance for large viscosity magnetic fluid, and by applying magnetic field. About 1.2 MPa of the maximum sealing performance at 5 μm of extremely tiny clearance is obtained for the test magnetic fluid C. Therefore, it was found that the sealing performance of the magnetic fluid is significantly enlarged in case of extremely tiny clearance such as 5 μm. This means magnetic fluid can be expected to apply the sealing fluid to the sliding parts of the compressor.

4. Results and discussion in Exp. 2

4.1. Data reduction

Figure 11 shows time-series variation of mass flow rate of magnetic fluid flow for 5 μm of clearance. The horizontal axis is elapsed time after the upstream pressure application and the vertical axis is the mass flow rate of the magnetic fluid flow. As mentioned in Sec. 2.2, because the setting channel height h is different from the actual channel height h', the actual channel height h' is determined by calibration with using the standard liquids for calibrating viscometers before each experiment. In this case, the setting clearance is 5 μm but the actual clearance is 9.16 μm. The theoretical mass flow rate can be calculated by the following Equation (1) with using h and h', represented in m_{set} and m_{act}, respectively.

$$m_{set} = \frac{\rho h^3 d}{12\eta l}\Delta p, \quad m_{act} = \frac{\rho h'^3 d}{12\eta l}\Delta p \tag{1}$$

where, $\rho, \eta, d, l, \Delta p$ are density, viscosity of the test magnetic fluid, channel width, length of flow path, and upstream pressure, respectively. The solid and dotted line respectively noted by m_{set} and m_{act} in Fig. 11 are the calculated mass flow rate from the Eq. (1). Fig.11 indicates that the measured mass flow rate without magnetic field has good agreement with m_{act}. Therefore, the actual channel height has reliability in this experiment. In addition, the measured mass flow rates are almost constant regardless of time and decreases by applying magnetic field.

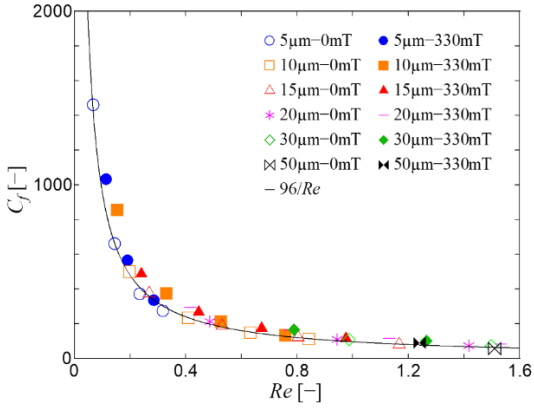

Fig. 12 Reynolds number dependence on frictional coefficient C¬f,exp without magnetic field and under magnetic field of 330 mT.

Reynolds number Re and frictional coefficient $C_{f,exp}$ can be derived by Equations (2) and (3), respectively.

$$Re = \frac{\rho u(2h')}{\eta} \tag{2}$$

$$C_{f,exp} = \Delta p \frac{2h'}{l} \cdot \frac{2}{\rho u^2} \tag{3}$$

The bulk mean velocity is obtained from the averaged value of the measured mass flow rate for 30 min and the actual channel height h'. The theoretical value of the frictional coefficient $C_{f,th}$ is given by Equation (4);

$$C_{f,th} = \frac{96}{Re} \tag{4}$$

4.2 Frictional coefficient

Figure 12 shows Reynolds number dependence on frictional coefficient $C_{f,exp}$ without magnetic field and under magnetic field of 330 mT. The solid line in this figure is the theoretical frictional coefficient $C_{f,th}$ calculated by Eq. (4). This figure depicts the frictional coefficient of the magnetic fluid flow without magnetic field almost corresponds to the theoretical values, because magnetic fluid can be treated as a Newtonian fluid without magnetic fluid. On the other hand, when the magnetic field is applied to magnetic fluid flow, $C_{f,exp}$ slightly increases compared with $C_{f,exp}$ without magnetic field. This is because the apparent viscosity increases by applying magnetic field. However, it is difficult to confirm the tendency in details from this figure. For better understanding and detailed discussion, the ratio of $C_{f,exp}$ to $C_{f,th}$ is calculated.

Figure 13 shows relationship between $C_{f,exp}/C_{f,th}$ and Reynolds number *Re* for (a) overall tendency, and extended figures (b) 5 and 10 μm, (c) 15 and 20 μm, (d) 30 and 50 μm. The $C_{f,exp}/C_{f,th}$ has naturally almost 1.0 under no magnetic field. However, when the magnetic field is applied to magnetic fluid, the value of $C_{f,exp}/C_{f,th}$ exceeds 1.0, and 1.4 of the maximum value of $C_{f,exp}/C_{f,th}$ is obtained at 5 μm the extremely tiny clearance as shown in Fig. 13(a). Figs. 13 (b)-(d) indicate that $C_{f,exp}/C_{f,th}$ drastically decreases with increasing *Re* for 5 and 10 μm of extremely tiny clearance, but the change in $C_{f,exp}/C_{f,th}$ with increasing *Re* becomes small for other channel height. It can be observed $C_{f,exp}/C_{f,th}$ tends to increase with increasing *Re* for other channel height except to 30 μm.

In order to clarify these complicated features of the magnetic fluid flow in tiny clearance, we analysed using the pressure force F_p acted on the cross-sectional area by upstream pressure and the frictional coefficient ratio with to without magnetic field $C_{f,mag}/C_{f,nomag}$. The pressure force F_p is defined as $F_p=\Delta p \cdot A=\Delta p \cdot dh'$, here, A is the cross-sectional area of channel. The relationship between F_p and $C_{f,mag}/C_{f,nomag}$ is shown in Fig. 14 for (a) overall tendency, and extended figures (b) 5 and 10 μm, (c) 15 and 20 μm, (d) 30 and 50 μm.

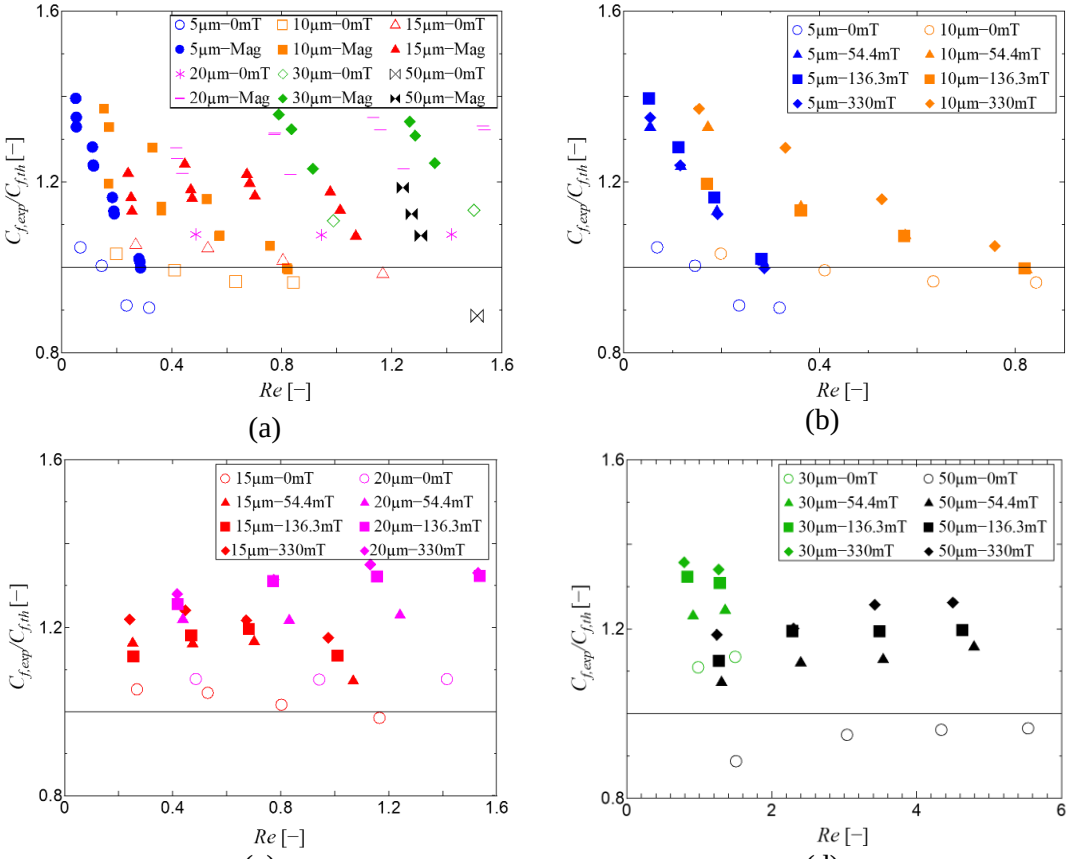

Fig. 13 Relationship between $C_{f,exp}/C_{f,th}$ and Reynolds number Re for (a) overall tendency, and extended figures (b) 5 and 10 μm, (c) 15 and 20 μm, (d) 30 and 50 μm.

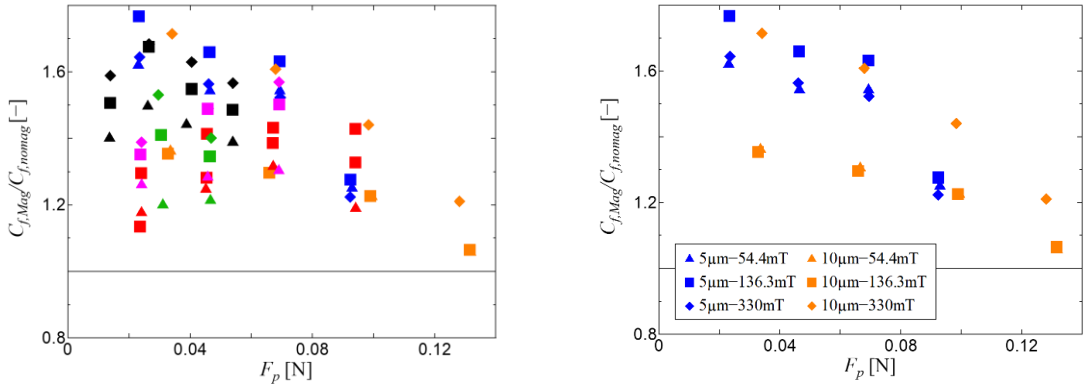

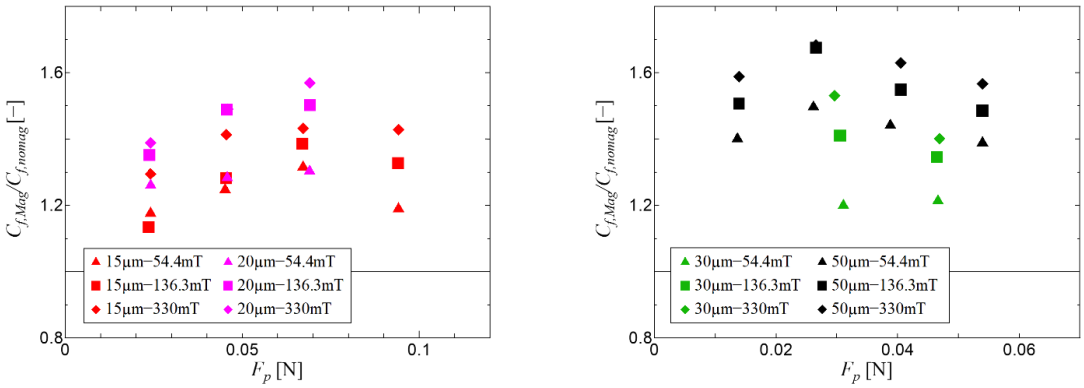

(c) (d)

Fig. 14 Relationship between F_p and $C_{f,mag}/C_{f,nomag}$ for (a) overall tendency, and extended figures (b) 5 and 10 μm, (c) 15 and 20 μm, (d) 30 and 50 μm.

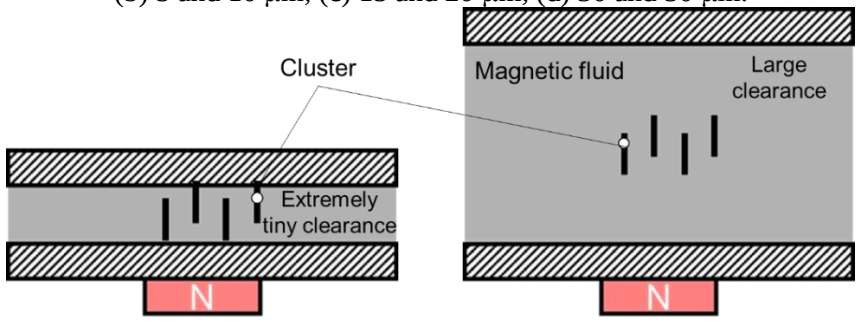

Fig. 15 Conceptual models of the influence of clustering structure in extremely tiny clearance and large clearance.

Figs. 14 (a) and (b) indicate that $C_{f,mag}/C_{f,nomag}$ has larger values under the same F_p and decreases with increasing F_p for extremely tiny clearances such as 5 and 10 μm compared with other clearances. About 1.8 of the maximum value of $C_{f,mag}/C_{f,nomag}$ is obtained at 5 μm of the extremely tiny clearance. This feature of frictional force corresponds to the largest pressure resistance for extremely tiny clearance like a sliding surface discussed in Exp. 1. On the other hand, when the clearance is 15 to 50 μm shown in Figs. 14(a), (c) and (d), $C_{f,mag}/C_{f,nomag}$ has the tendency to increase with increasing F_p, and large $C_{f,mag}/C_{f,nomag}$ is also obtained in large channel height such as 50 μm. Tomita et al. [11] investigated the effect of clearance on the frictional coefficient of magnetic fluid in channels which has several millimetres of channel height, and reported that the frictional coefficient increases with increasing the channel height. Similar tendency is obtained in our experiment for large clearance more than around 15 μm.

Generally, it is well known that when the magnetic field is applied to the magnetic fluid the viscosity of magnetic fluid increases apparently and the inner magnetic particles agglomerate and form the clustering structures in the direction of magnetic field. In addition, the clustering structure grows under the static condition, but the clustering structure is difficult to grow largely under the flowing condition. Both increase of apparent viscosity and the formation of the clustering structure seem to have strong influence on the frictional coefficient. Fig. 15 represents the conceptual models of the influence of clustering structure

in the extremely tiny clearance and large clearance. In case of large clearance more than around 20 μm, as the size of clustering structure is much smaller than the clearance, the influence of clustering structure should be weak and frictional coefficient increase by the effect of increase of apparent viscosity. However, in the case of extremely tiny clearance such as 5 and 10 μm, it seems that both the formation of clustering structure and increase of apparent viscosity effect on the increase of frictional coefficient in the clearance (e.g. pressure resistance).

5. Conclusion

Sealing performance and flow characteristics of magnetic fluids in extremely tiny clearance less than 10 μm and small clearance such as 15-50 μm are investigated experimentally. Two experiments which are searing performance experiment as Exp. 1 and flow characteristic experiment as Exp. 2 are performed. The following result are obtained in both experiments.

In Exp. 1, the better sealing performance is obtained in the narrower clearance and larger viscosity magnetic fluid with applying magnetic field. Especially, the pressure resistance drastically increases in the extremely tiny clearance such as 5 μm by applying magnetic field. About 1.2 MPa of the maximum sealing performance at 5 μm of extremely tiny clearance for the test magnetic fluid C. This means magnetic fluid can be expected to use the sealing fluid to the sliding parts of the compressor.

In Exp.2, when the magnetic field is applied to magnetic fluid flow, frictional coefficient of magnetic fluid flow slightly increases compared with that without magnetic field. For better understanding this feature in detail, we discuss the relationship between the pressure force acted on the cross-sectional area by upstream pressure and the increasing ratio of frictional coefficient with to without magnetic field. In case of extremely tiny clearance such as 5 and 10 μm, the increasing ratio has larger value comparing with other clearance, and tends to decrease with increasing pressure force. On the other hand, in large clearance more than 20 μm, the increasing ratio tends to increase with increasing pressure force, and large value is also obtained in largest clearance of 50 μm.

References

[1] J. Philip et al., Enhancement of thermal conductivity in magnetite based nanofluid due to chainlike structures, Appl. Phys. Lett., 91, 2007, 203108.

[2] M. Chouhan et al., An investigation on the optimization of anti-wear performance of nano-Fe3O4 based ferro-magnetic lubricant, J. Tribologi, 25, 2020, 119-135 .

[3] S. Miyake, Applications of Magnetic Fluid Seals to Vacuum, Shinku, 28, 1985, 483–493. (in Japanese)

[4] Y. Mizutani et al., Magnetic fluid seal for linear motion system with gravity compensator, Procedia CIRP, 33, 2015, 581-586.

[5] K. van der Wal et al., Ferrofluid rotary seal with replenishment system for sealing liquid, Tribology Int., 150, 2020, 106372.

[6] X. Li et al., Optimal design of large gap magnetic fluid sealing device in a liquid environment, J. Magn. Magn. Mater., 540, 2021, 168472.

[7] L. Jiang et al., Experimental investigation on the critical pressure and self-repairing capability of conversing magnetic fluid seal with stepped pole pieces, Tribology Int., 185, 2023, 108506.

[8] Y. Mitamura, A magnetic fluid seal for implantable blood pumps: Structure for a long life, J. JSAEM, 27, 2019, 280-285. (in Japanese)

[9] JSRAE, Compressors for Air Conditioning and Refrigeration, JSRAE Technical Books Series, 2018, 91.

[10] M. Fukuta et al., Seal mechanism of tip seal in scroll sompressor, Proc. Purdue Conf., 2014, 2292.

[11] Y. Tomita et al. Flow behavior of ferrofluid in a two-dimensional channel (2nd report, effects of concentration, channel feight and intensity of applied magnetic field), Tran. JSME B, 57, 1991, 59-65. (in Japanese)